Chapter 6

Self-Protected Sensor System Utilizing Fiber Bragg Grating (FBG)-Based Sensors

Chien-Hung Yeh and Chi-Wai Chow

Additional information is available at the end of the chapter

http://dx.doi.org/10.5772/57417

1. Introduction

Utilization of fiber Bragg gratings (FBG) to serve as the fiber-optic sensors are important researches for the optical fiber sensing applications [1–4]. Hence, when the strain or temperature variations are imposed on the FBG-based sensor, the Bragg wavelength will drift due to the index change of the FBG, and thus the detected wavelength will also shift. And so, according to the wavelength shift phenomenon of FBG, we could easily observe the strain and temperature variations for sensing [3]. In the distributed fiber sensors of the intelligent sensing network system, the FBG-based sensor has been studied and identified as an important sensing element for sensing the change of temperature and strain [1–6]. Hence, the large-scale FBG sensor system could be built and achieved easily by wavelength multiplexing technology [7–9].

During the strain sensing, if the payload applied on the FBG is over its limitation, FBG breakage will occur. Furthermore, the fiber-fault of FBG-based sensing network also could affect the survivability and reliability. As a result, how to improve and enhance the reliability and survivability of sensor network becomes the essential issue for further study. To keep the survivability of an FBG sensor system against fiber fault, a few self-protection schemes have been reported [10,11]. However, these methods required optical switch (OSW) in each remote node (RN) to re-route the sensing path for detecting and protecting the fiber fault. It was hard to control and judge the direction of OSW in each RN and also increased the complexity and cost of FBG-sensor networks. In addition, even though these FBG sensor systems were passive sensing networks in multi-ring schemes in the past studies [1, 2]. But, these ring sensor architectures required many numbers of RNs, consisting of optical coupler (OCP), to produce multi-ring configurations and result in the huge fiber connect points to reduce the power budget after run trip transmission.

In this work, we will introduce two different FBG-based sensor networks utilizing the passive system design. In the first design, a self-protected passive FBG sensor network, which enhances the reliability and survivability in long-reach fiber distance, is proposed and experimentally investigated. The sensing mechanism is based on a 25 km cavity length erbium-doped fiber (EDF) ring laser for detecting the multiple FBG sensors in the network. And we only use an optical coupler (OCP) on RN to produce multi-ring configuration. The advantage of the proposed fiber laser scheme for detecting and monitoring the FBG sensors in the long distance self-protected scheme can facilitate highly reliable and survivable operation. Besides, the long distance sensing system can be integrated in fiber access network to reduce the cost of sensor infrastructure in the future. In the second design, we propose and demonstrate a multi-ring passive sensing architecture, which does not have any active components in the entire network. In this experiment, the network survivability and capacity for the multi-point sensor systems are also enhanced. Moreover, the tunable laser source (TLS) is adopted in central office (CO) for FBG sensing. The survivability of an eight-point FBG sensor is examined and analyzed. Due to the passive sensor network, the cost-effective and intelligent sensing system is entirely centralized by the CO. As a result, the experimental results show that the proposed system can assist the reliable FBG sensing network for a large-scale and multi-point architecture.

2. First FBG sensor network architecture

The proposed LR self-healing FBG-based sensor system was consisted of a central office (CO) and multiple sensing networks, as shown in Figure 1. Here, two 25 km long single-mode fibers (SMFs) were used to connect to the CO and a N×N optical coupler (OCP), which was located at remote node (RN). The upper (path "1") and lower SMFs (path "2") were used to serve as the feeder fibers for sensing signal transmission. The N×N OCP could produce N×1 fiber ring architectures. And each ring scheme could use M FBGs for system sensing. A wavelength-tunable laser (WTL) source was used to detect and monitor the FBG sensors in the CO. For the initial deployment of the sensing network, the power budget (i.e. the power of the laser source and the split-ratio of the sensing network) should be carefully considered. If the power budget is not enough due to high split ratio, fiber amplifiers between CO and RN can be used to solve this issue. Besides, according to current passive access network standards [12], this proposed 25 km long sensor system can be also integrated in the fiber access system to enhance the use of capacity fiber and reduce the cost of sensor infrastructure.

To realize and perform the proposed FBG-based sensor network, the experimental setup was performed on a simplified version as illustrated in Figure 2. The CO was constructed by a WTL, a 1×2 OSW and an optical spectrum analyzer (OSA). In this measurement, the WTL was consisted of an erbium-doped fiber amplifier (EDFA), a tunable bandpass filter (TBF), a 4×4 OCP, a polarization controller (PC), a variable optical attenuator (VOA). The 980 nm pumping laser of EDFA operated at 215 mA and the saturated output power of the EDFA was around 16 dBm at 1530 nm. The tuning range, insertion loss and 3 dB bandwidth of TBF used was 36 nm (1526 to 1562 nm), <0.7 dB and 0.3 nm, respectively. The PC and VOA were used to control and adjust the polarization status and maintain the maximum output power. Therefore, the

http://dx.doi.org/10.5772/57417

4×4 OCP would introduce three ring sensing networks. And the two feeder fibers were 25 km long. In the experiment, the sensor network has eight FBGs, which could be used for the strain and temperature sensing applications. Moreover, the Bragg wavelengths of these FBGs, which have different reflectivity, were 1527.6 (λ_{11}), 1528.9 (λ_{12}), 1532.9 (λ_{21}), 1536.7 (λ_{22}), 1538.4 (λ_{23}), 1541.7 (λ_{31}), 1546.0 (λ_{32}) and 1556.0 nm (λ_{33}), respectively.

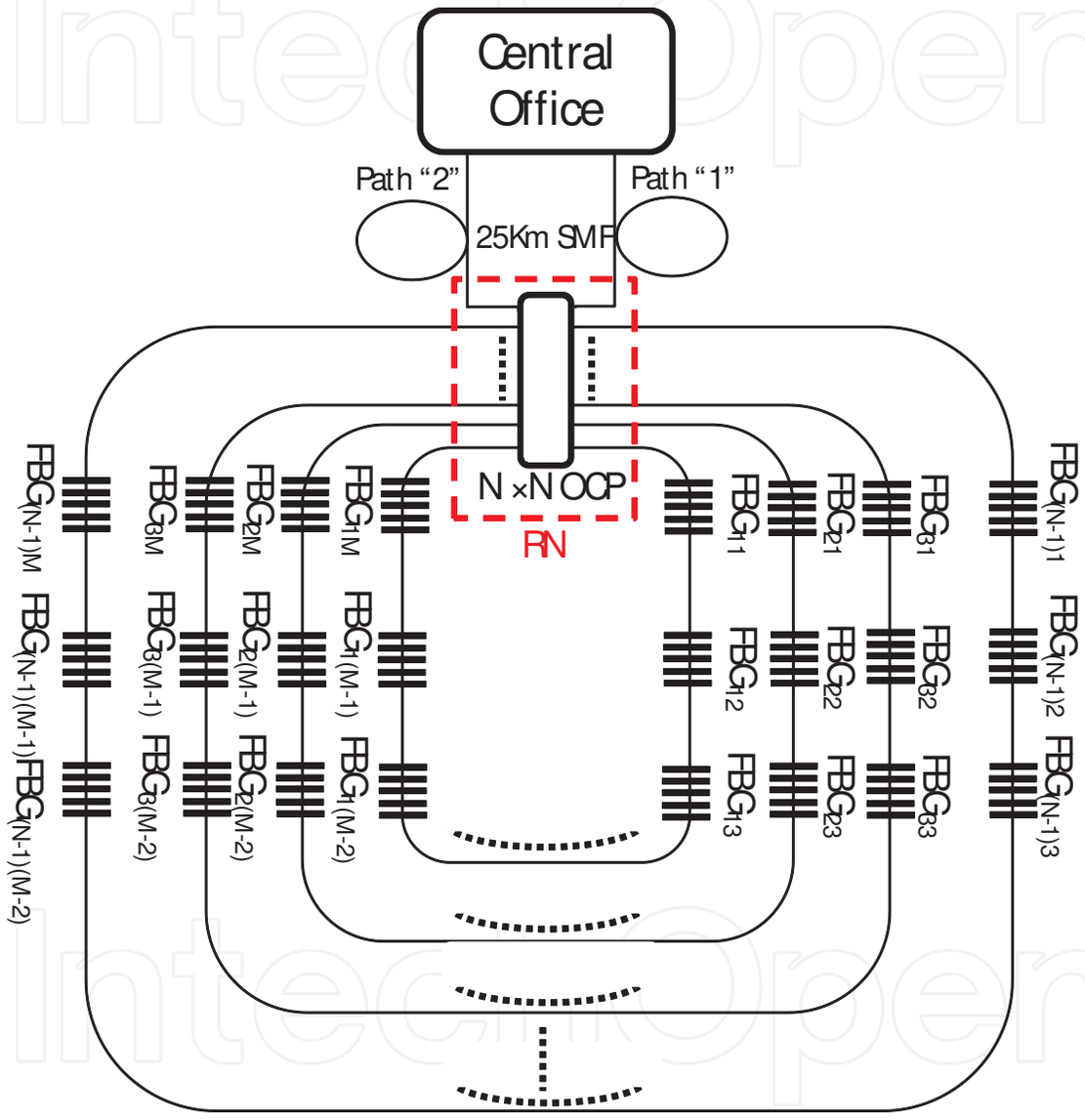

Figure 1. Proposed long distance FBG sensor system in passive multi-ring architecture. SMF: single-mode fiber; OCP: optical coupler; FBG: fiber Bragg grating; RN: remote node.

The proposed WTL scheme in CO contained the C-band erbium-doped gain operation. And the passband of the TBF, using inside gain cavity, was scanned to match the corresponding Bragg wavelength of FBG. Each FBG element served as the reflected sensor head and was connected as the part of cavity via a 25 km long fiber. Due to the inclusion of the TBF within the cavity loop, the lasing wavelength would be generated only when the filter passband was

aligned in accordance with one of the FBG elements. In normal operation, when the TBF was set at one of the Bragg wavelength of the FBG, a long cavity fiber ring laser will be formed, and a lasing wavelength will be detected at the OSA located in the CO, with a 0.05 nm resolution.

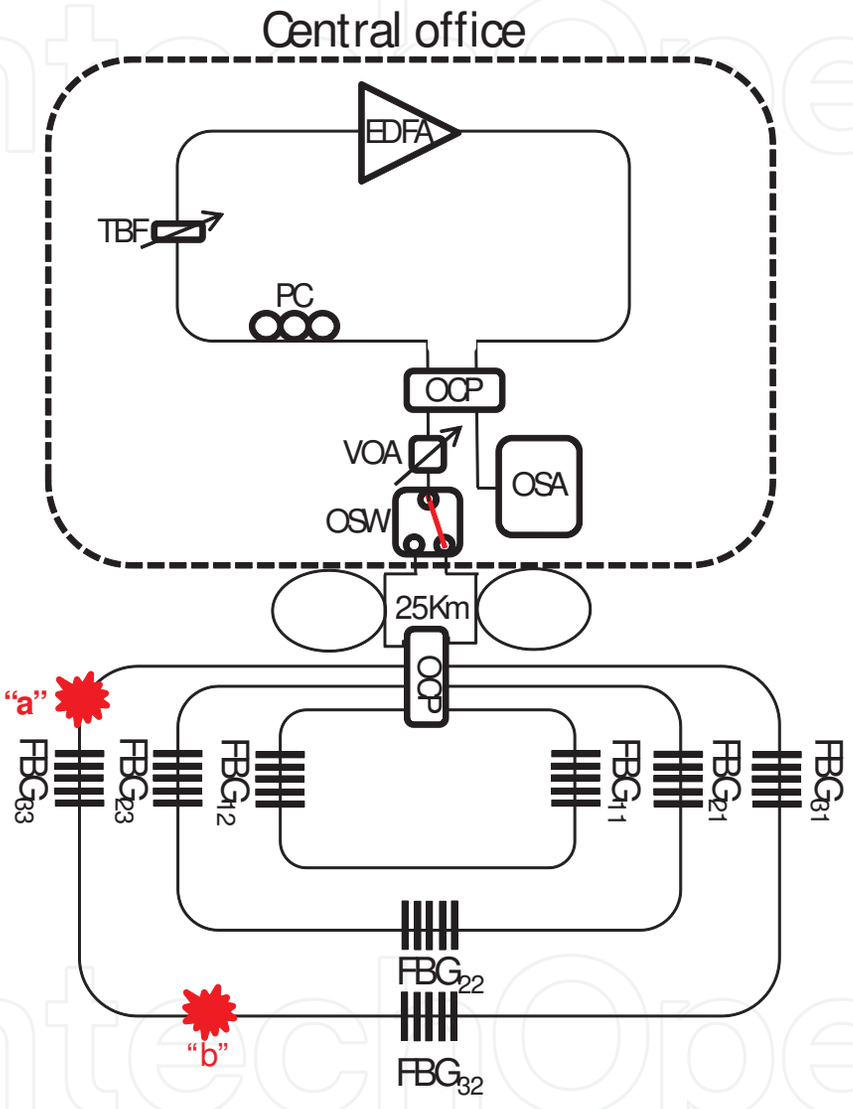

Figure 2. Experimental setup of proposed long distance self-healing FBG-based sensor system.

Initially, the OSW of CO was located on position "1" to connect to the sensor network via the upper feeder fiber (path "1") for detecting and monitoring the eight FBG sensors used, as illustrated in Figure 2. Here, Figure 3(a) shows the reflected wavelengths of the proposed FBG-based sensor network from 1527.6 to 1556.0 nm (λ_{11} to λ_{33}) via upper fiber. Here, we can observe eight lasing wavelengths in Figure 3(a) using the proposed WTL scheme during the TBF scanning. Of course, we could also connect the FBG sensor network for via the lower feeder fiber (path "2"), when the 1×2 OSW was switched to position "2", as shown in Figure 2. Hence,

http://dx.doi.org/10.5772/57417

Figure 3(b) presents the retrieved output wavelengths of the eight FBG sensors system via the lower feeder fiber. As shown in Figure 3(a) and Figure 3(b), no matter from which fibers to transmit the detecting signal to monitor FBG sensors, the measured reflective wavelengths are the same. However, the obtained wavelength λ_{11} of Figure 3(b) is slightly drifted due to the different forward and backward reflected spectrum of FBG_{11}. As a result, we can switch the direction of OSW for connecting the upper or lower feeder fibers to monitor the status of FBG sensors and each ring fiber simultaneously.

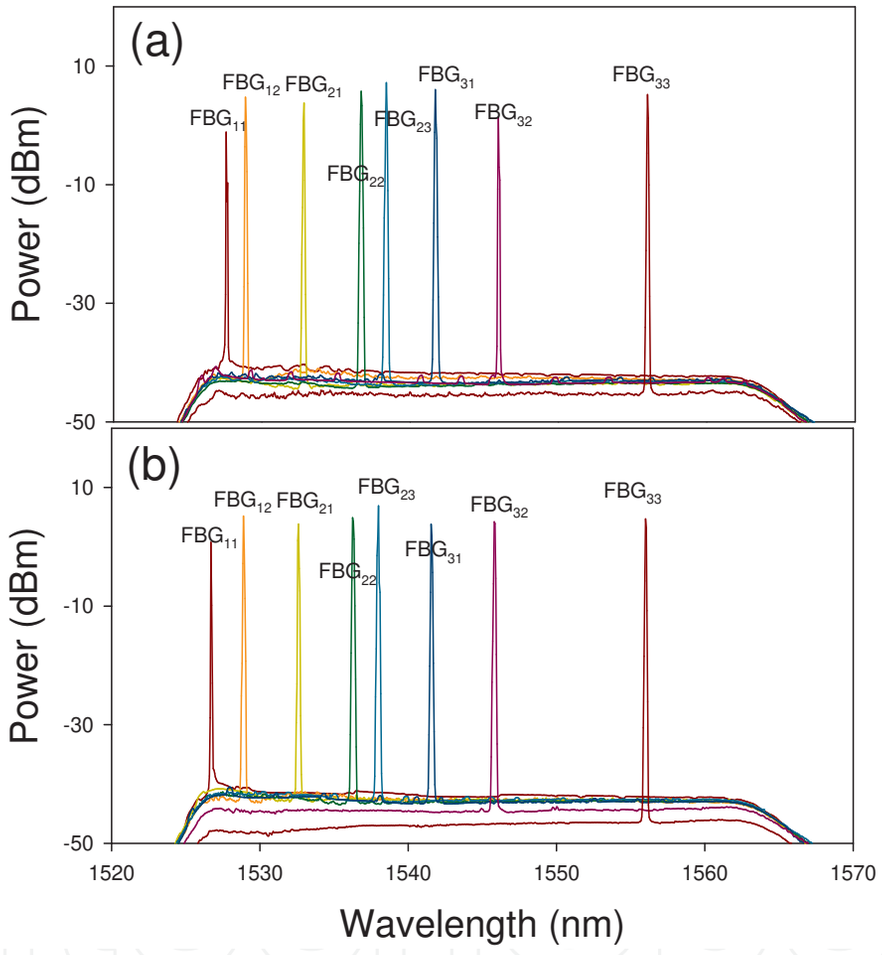

Figure 3. Output wavelengths of the proposed FBG-based sensor system from 1527.6 to 1556.0 nm via the (a) working and (b) protecting fiber links.

In the first scenario, the fiber fault may happen inside the fiber ring network. Hence, if a fiber cut occurs at point "b", as seen in Figure 2, the lasing wavelengths of λ_{32} and λ_{33} can be not measured via the upper feeder path, as shown in Figure 4(a). At this moment, the OSW will switch to position "2" to connect the lower feeder fiber for rescanning the FBG sensors. Thus, only the wavelength λ_{31} can be not retrieved by the proposed WTL scheme, as illustrated in Figure 4(b). According to the measured results of Figure 4(a) and Figure 4(b), then we can locate and ensure the cut position among FBG_{31} and FBG_{32}. Besides, if two fiber cuts occur at

point "a" and "b" simultaneously in the sensor network, the lasing wavelengths of λ_{31}, λ_{32} and λ_{33} via the paths "1" and λ_{31} via the path "2" can be not measured by OSA, respectively. Hence, we can ensure the faults are among points "a" and "b". Furthermore, when the external strain is applied on FBG_{31} before broking, the wavelength shifts can be observed, as illustrated in Figure 5. Here, the maximum strain shift of FBG_{31} is nearly 2.2 nm. When the temperature of FBG increases gradually, the reflected wavelength of the FBG will shift. In the proposed FBG sensing network, certain sub-ring systems could be used for the temperature sensing. Besides, some FBG sensors are used for both temperature-sensing as well as fiber-cut location detection. In the measurement, the maximum wavelength shift of FBG_{31} is ~2.2 nm when the temperature of FBG_{31} change is around 68 °C. While the strain exceeds the limitation of FBG31, the FBG sensor will be broken. In such situation, if a fault occurs on FBG_{31}, the measured lasing wavelengths in CO are the same comparing with the results of Figure 4. However, we can first observe the wavelength drift before FBG broking. As a result, we can clearly know the differences of fiber-fault and FBG-fault in the proposed passive FBG sensor network.

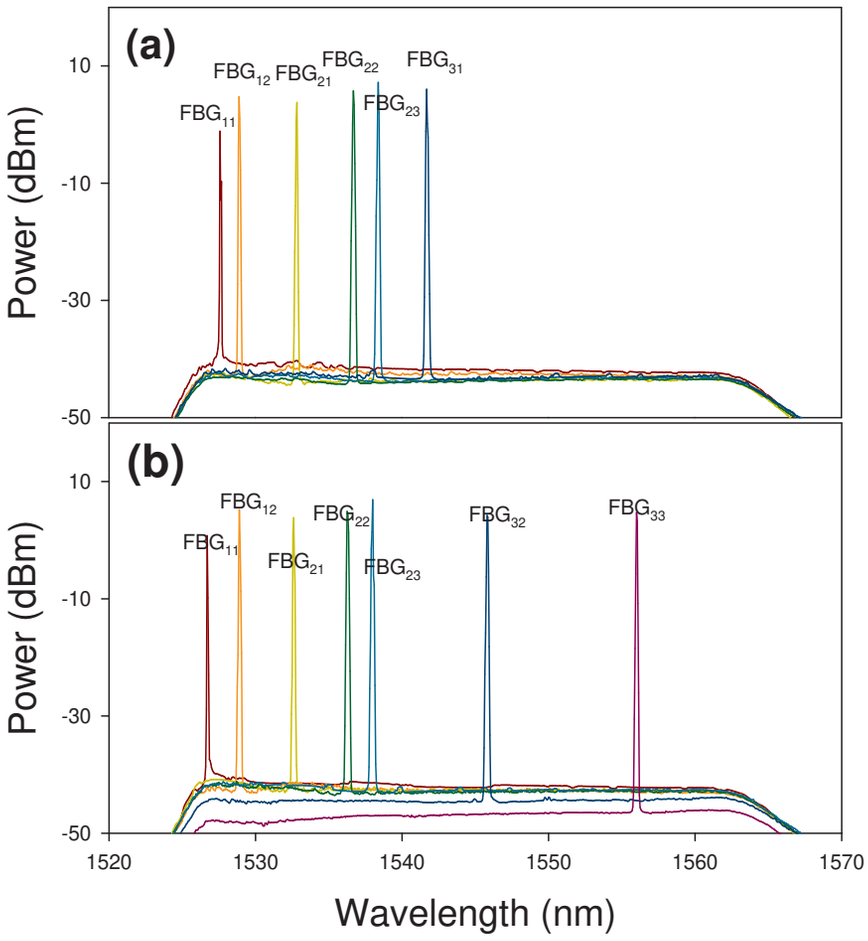

Figure 4. Output wavelengths of the proposed FBG-based sensor system via the (a) working and (b) protecting fiber links, when a cut occurs at "b" point in Figure 2.

http://dx.doi.org/10.5772/57417

In addition, it is necessary to ensure that each FBG sensor was in good situation in fiber sensor system. Thus, when the strain or temperature change was applied on each FBG sensor due to the environmental or artificial effect, the sensor will cause the Bragg wavelength shift. For the second scenario, while the payload of the FBG exceeds the limitation, the FBG would be broken. Here, the proposed ring sensor architecture also could find the position of the broken FBG. For example, if the FBG_{22} was broken in the proposed sensor network via the fiber path "1", the lasing wavelengths of λ_{22} and λ_{23} would not be detected, as shown in Figure 6(a). Hence, to detect the disappeared FBG sensors, the CO would control the OSW to reconnect to the lower feeder fiber (path "2") for sensing FBG. Thus, the measured output spectrum lacks the λ_{21} and λ_{22}, as shown in Figure 6(b). Comparing the two output spectra of Figurs 6(a) and 6(b), we can easily locate the fault is on FBG_{22}. Moreover, for example, when the measured lasing spectra of the λ_{11}, λ_{12}, λ_{21}, λ_{22} and λ_{23} via the fiber path "1", and λ_{11} and λ_{21} via the fiber path "2" respectively, are not detected by the proposed sensor system, we can assure that two sensors of FBG_{11} and FBG_{21} are broken at this time.

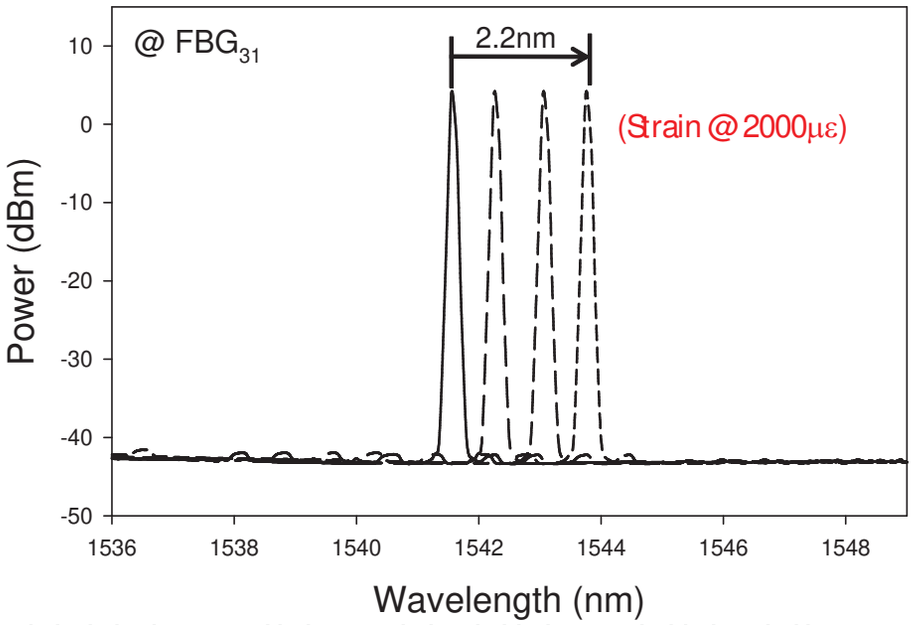

Figure 5. Reflected spectrum of FBG_{31} when the strain is applied.

We can be according to the above measured methods to ensure when the sensing path is via the feeder fiber paths "1" and "2". Initially, we can observe entire reflected wavelengths of FBG sensors via feeder path "1" when this sensing network is without FBG fault or fiber fault. When a fault is produced on FBG_{xy}, first we can observe that the reflective-wavelength of measured FBG_{xy} should be shift and then broken. Based on the measured result, we can realize the fault which is on FBG not on fiber. Besides, when the occurrence of fiber fault is produced, the all observed reflective-wavelengths are no change at this time. As a result, the proposed FBG sensor system not only can find out the fiber fault, but also detect and monitor the FBG sensors.

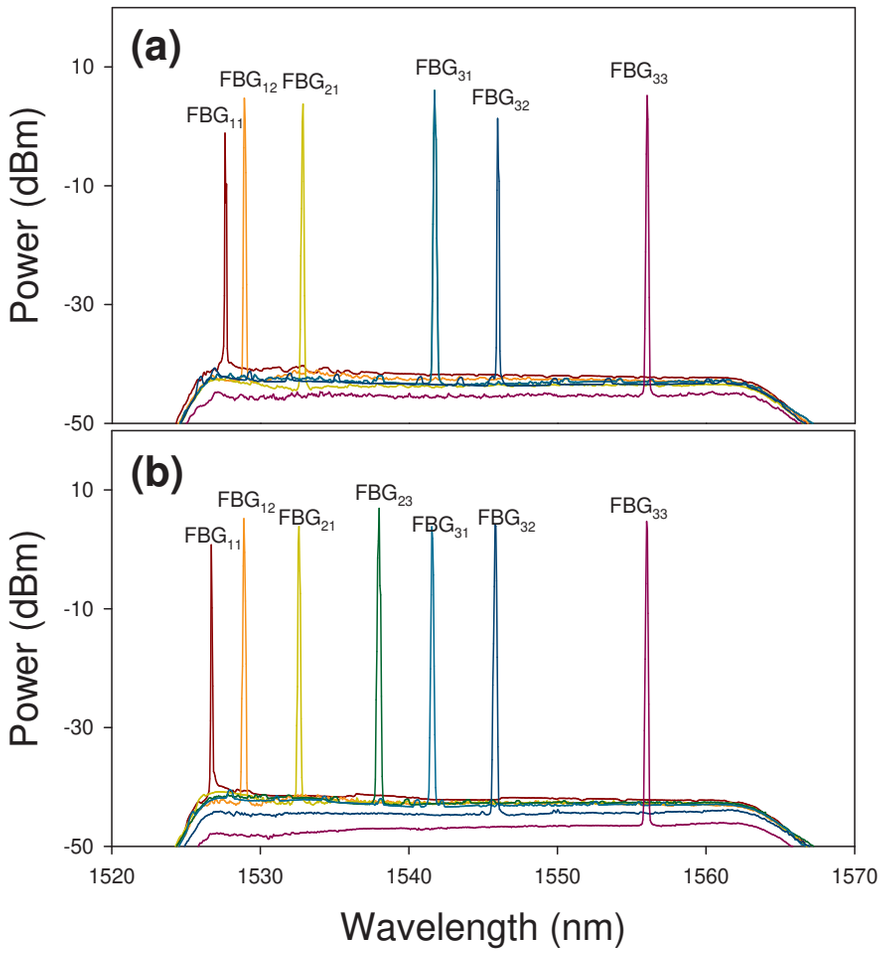

Figure 6. Measured output spectra of the sensing system via the (a) upper and (b) lower feeder fibers while a fault is on FBG_{22}.

3. Second FBG sensor network architecture

Figure 7 shows the simply self-restored ring-based architecture for passive FBG sensor system. The central office (CO) is constructed by a tunable laser source (TLS), an optical circulator (OC), a 1×2 optical switch (OS). Two output ports of OS are used to circulate a major ring. Besides, the 1×2 OS can be used to select the fiber path "a" or "b" for the sensing transmission. Assuming there are m sub-ring sensor groups in the major ring sensing system and the each groups have n FBG sensors, as illustrated in Figure 7. Each remote node (RN) uses a 2×2 optical coupler (C) to circulate sensor group and also connect next sensor group. Thus, the proposed sensing system has (m×n) FBG sensors. The sensing laser source usually uses linear-cavity erbium-doped fiber (EDF) ring laser for fiber sensor because the laser has intense output power and high OSNR [13]. In our proposed sensing network, the TLS is distributed to each RNs and delivered to each FBG sensor through each sensor groups. The TLS has the advantage of high

http://dx.doi.org/10.5772/57417

output power and optical signal to noise ratio (OSNR) to detect the FBG sensor in the network. In the sensing network, three fault locations could occur, such as in the major ring, sub-ring, and fiber sensor itself. In the following analysis, we will discuss and analyze the three situations based on the simply apparatus and ring-based architecture.

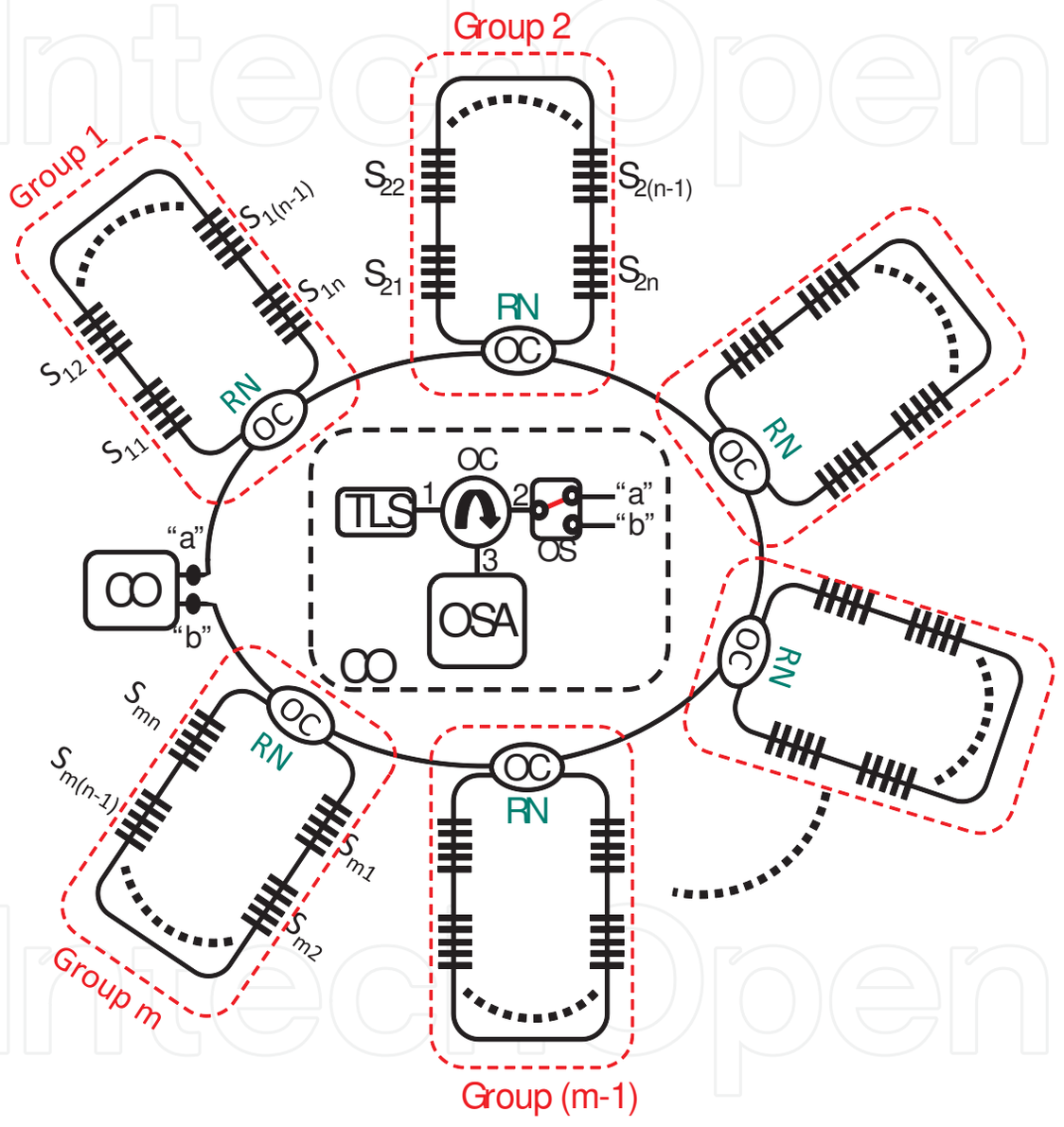

Figure 7. Proposed simply self-restored ring-based architecture for passive FBG sensor system. S: sensor, C: coupler, CO: central office, RN: remote node, OS: optical switch, OC: optical circulator, OSA: optical spectrum analyzer.

To realize and evaluate our proposed self-restored ring-based architecture for passive FBG sensor system, a simply experimental setup is shown in Figure 8. In the sensing system, the m and n of the setup are equal to four and two in the experiment. That is to say, there are eight FBG sensors (S_{mn}) using in the sensing network experiment. Each of the sensing FBGs (S_{11} to

S_{42}) are used to act as the reflected elements. In the CO, the lasing of TLS is detected by these FBGs. The Bragg wavelengths of the eight FBGs used are 1526.63, 1528.87, 1532.64, 1536.57, 1538.24, 1541.88, 1545.83 and 1555.85 nm, respectively. In addition, the fiber sensing system can also be used to accurately measure the strain and temperature perturbations applied on the FBGs. In normal status, the OS locates at point "1" to connect the path "a". Thus, the lasing wavelength from CO passes through the path "a" to detect FBG sensors. As illustrated in Figure 8(a), the green arrows show the sensing transmission path when the sensor system link without any faults. Figure 8(b) also shows the received output spectra of the eight sensing sensors from S_{11} to S_{42} by using the TLS while the sensing transmission through the path "a". When there is no fiber fault in the network, the CO would detect the eight fiber sensors in the proposed sensing system.

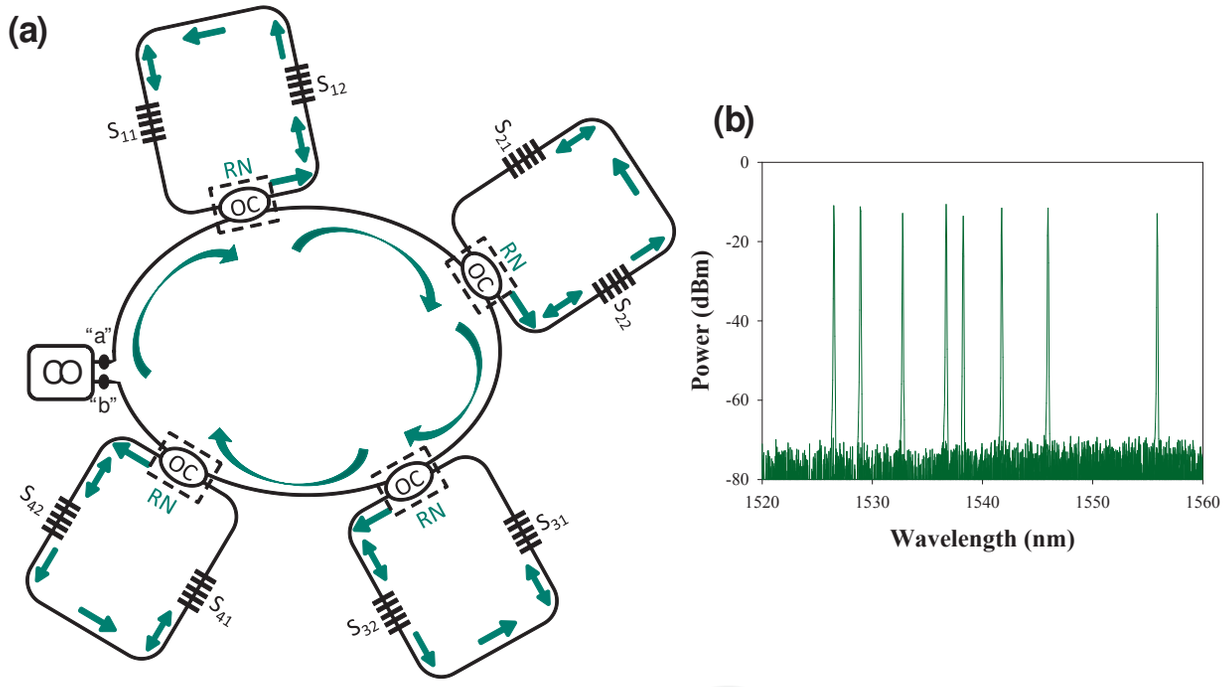

Figure 8. (a) Experimental setup for the self-restored passive FBG sensor system with eight FBS sensors from S_{11} to S_{42} without any fails. (b) Received output sensing spectra from the eight sensing FBGs in CO. (Green arrow presents the sensing transmission of the proposed network)

First, the sensor system passes through the path "a" initially for fiber sensing without any faults. When the proposed sensor network has a fiber cut on major ring between the group "2" and "3", as shown in Figure 9(a), the CO can only detect the received output sensing spectra from S_{11} to S_{22} (as seen in green line), as shown in Figure 9(b). In order to detect the residual FBG sensors, the OS could switch automatically to point "2" to link the fiber path "b". The sensing transmission is shown in red arrow, as also illustrated in Figure 9(a). When the sensing transmission is switched to path "b", the residual output sensing spectra from other sensors [as seen in red line of Figure 9(b)] can be detected. As a result, in accordance with the proposed operating mechanism, the self-restored ring-based sensor system could be protected from fiber fault on major fiber and detects the fault location approximately. If two fiber cuts are between

http://dx.doi.org/10.5772/57417

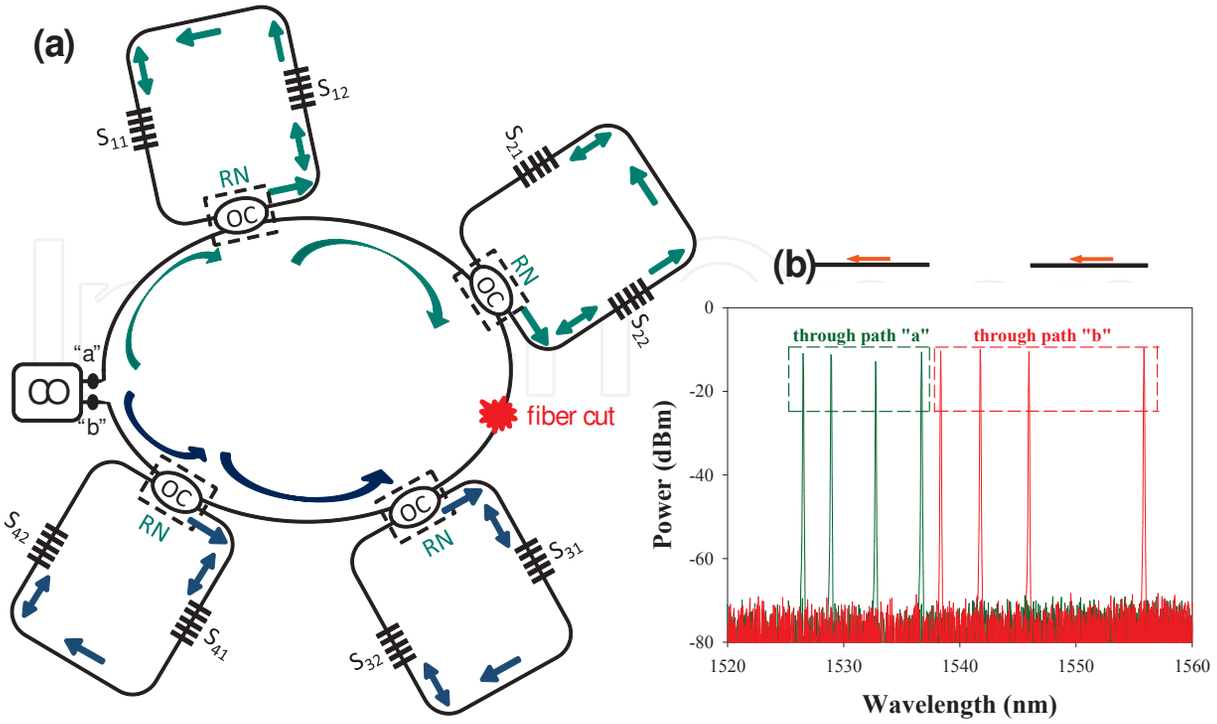

Figure 9. (a) When the sensor system has a fiber cut on major ring between the group "2" and "3" in the proposed sensing network. (b) Received output sensing spectra of the eight sensing FBGs in CO. (Green and red lines represent the sensing transmission through path "a" and "b", respectively.)

the group "2" and "3" and the group "3" and "4" in Figure 8, respectively, then the sensor S_{31} and S_{32} cannot be detected due to the two faults. However, the probability of producing two fiber faults simultaneously is very low in real sensing system.

And then, we will discuss and experiment the fiber fault in sub-ring sensor group as follows. When a fiber cut occurs between S_{21} and S_{22} in sensor group "2" through the path "a", as shown in the above of Figure 10(a), the proposed sensing network cannot detect the sensor S_{21}. Hence, as shown at the top of Figure 10(b), the output sensing spectrum lacks the sensor S_{21}. At the same time, the CO would control the OS to connect to the transmission path "b", as illustrated at the bottom of Figure 10(a). At the bottom of Figure 10(b), the output spectrum of sensor lacks the information of S_{22}. Therefore, compared with the two output sensing spectra of Figure 10(b), it can be easy to find out the fault location by detecting the FBG sensors information in the proposed network.

In sensor system, it is necessary to ensure that each fiber sensor is in good condition. Thus, when the strain or temperature change applied on FBG due to the environment or artificial effect, the fiber sensor would cause the Bragg wavelength shift. While the payload of the FBG exceeds the limitation, the FBG would cut. So, the proposed sensing system also can look for the position of broken sensor. For example, while the sensor S_{22} is broken in the proposed sensing network through the fiber path "a", the sensing network cannot detect the sensor S_{22}

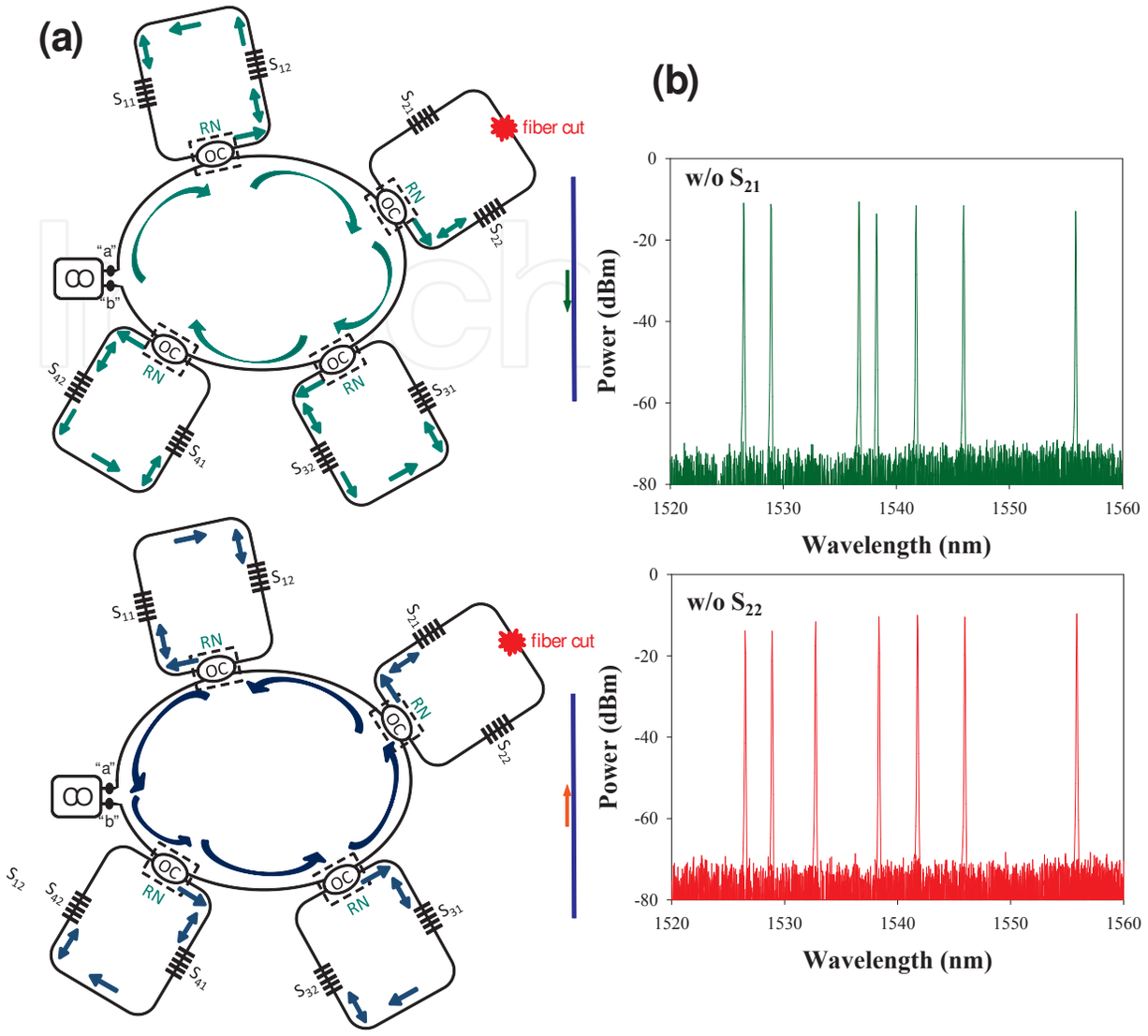

Figure 10. (a) When the sensor system has a fiber cut on sub-ring sensor group "2" in the proposed sensing network. (b) Received output spectra of the eight sensing FBGs in CO. (Green and red lines represent sensing information through the path "a" and "b", respectively.)

and sensor S_{21}, as shown at the top of Figure 11(a). Thus, at the top of Figure 11(b), the output sensing spectrum lacks the sensor S_{22} and sensor S_{21}. To obtain and detect the disappeared sensors, the CO would control the OS to connect the transmission path "b", as illustrated at the bottom of Figure 11(a). At the bottom of Figure 11(b), the output spectrum of sensor information lacks a sensor S_{22}. Then, by comparing the two output sensing spectra of Figure 11(b), we can easily find out that the fault is on sensor S_{22}. Besides, if two sensors of S_{22} and S32 are cut, the measured output spectra would lack the sensor S_{21}, S_{22}, S_{31}, and S_{32} through the path "a". When the sensing path passes through the path "b", the measured output spectrum would lack the sensor S_{22} and S_{32}. As a result, this proposed sensing network can find out two or more sensor cuts.

http://dx.doi.org/10.5772/57417

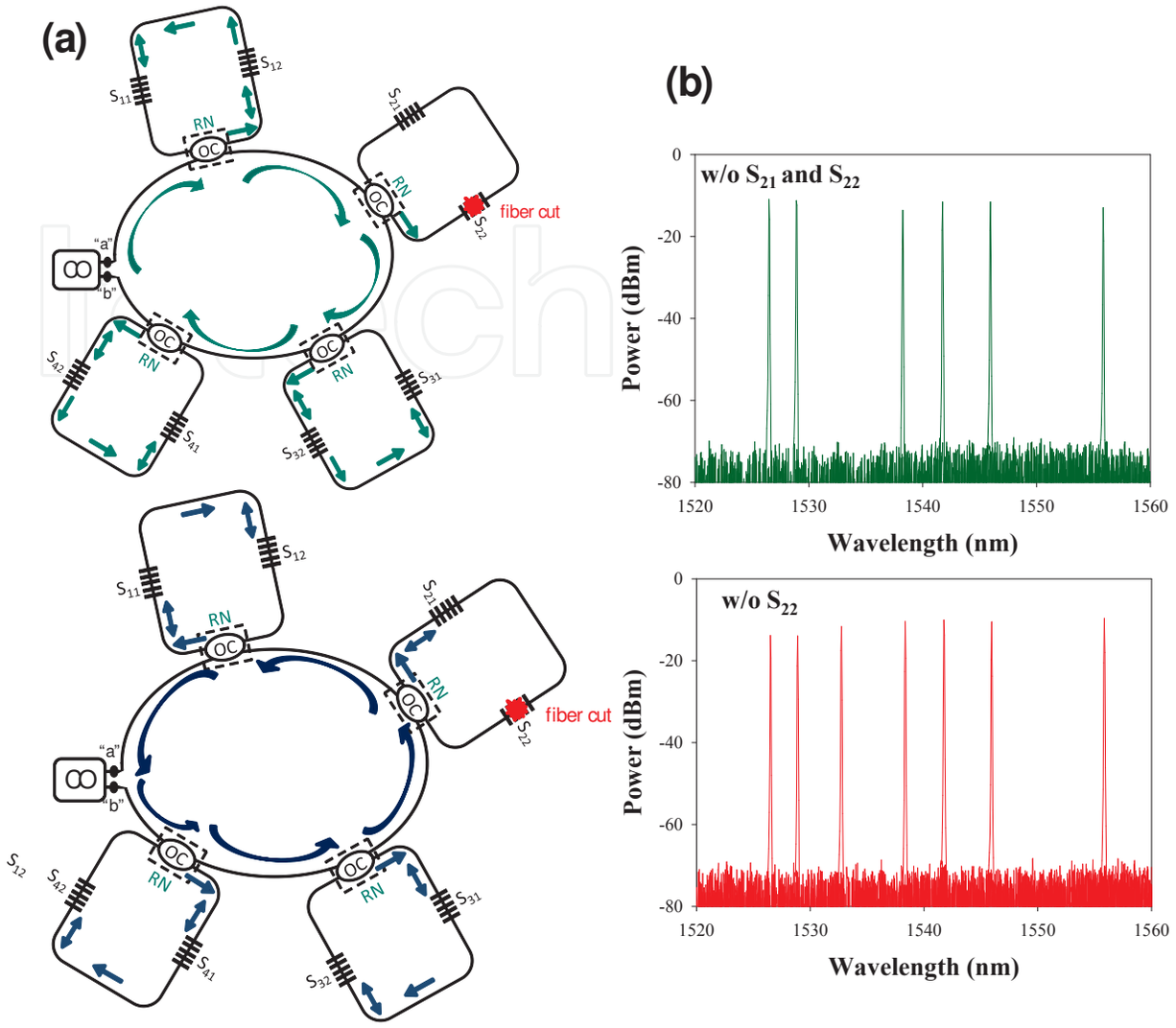

Figure 11. (a) When the sensor system has a fiber cut on the sensor S22 in the proposed sensing network. (b) Received output spectra of the eight sensing FBGs in CO. (Green and red lines represent sensing information through the path "a" and "b", respectively.)

4. Conclusion

In summary, in first proposed design, we have proposed and experimentally investigated a simple self-restored FBG based sensor ring system for long distance sensing. Besides, there is no active component in the FBG sensor architecture for cost reduction. The sensing mechanism is based on a 25 km cavity length EDF ring laser for detecting the multiple FBG sensors in the network. In this experiment, three scenarios of fault detections were experimentally studied, showing that the sensing network survivability, reliability and capacity for the multiple sensors can be enhanced. In the future, this proposed sensing network can be integrated into a fiber access network for advanced applications. And in second proposed design, we have proposed and experimentally investigated a simply self-restored FBG based sensor ring system. There are no active components in the entire sensing architecture. In this experiment,

the network survivability and capacity for the multi-point sensor systems are also enhanced. Besides, the TLS is adopted in CO for FBG sensing. The survivability of a eight-point FBG sensor is examined and analyzed. Due to the passive sensor network, the cost-effective and intelligent sensing system is entirely centralized by the CO. As a result, the experimental results show that the proposed system can assist the reliable FBG sensing network for a large-scale and multi-point architecture.

Author details

Chien-Hung Yeh[1] and Chi-Wai Chow[2]

1 Information and Communications Research Laboratories, Industrial Technology Research Institute (ITRI), Chutung, Hsinchu, Taiwan

2 Department of Photonics, National Chiao Tung University, Hsinchu, Taiwan

References

[1] Yeh, C. H., Chow, Chow, C. W., Wang, C. H., Shih, F. Y., Wu, Y. F., and Chi, S. A simple self-restored fiber Bragg grating (FBG)-based passive sensing network. Measurement Science and Technology 2009; 20(4) 043001.

[2] Yeh, C. H., Chow, C. W., Wu, P. C., and Tseng, F. C. A simple fiber Bragg grating-based sensor network architecture with self-protecting and monitoring functions. Sensors 2011; 11(2) 1375−1382.

[3] Peng, P. C., Tseng, H. Y., and Chi, S. (2002): Fiber-Ring Laser-Based Fiber Grating Sensor System Using Self-Healing Ring Architecture. Microwave and Optical Technology Letters 2002; 35(6) 441-444.

[4] Zhang, B., and Kahrizi, M. High-temperature resistance fiber Bragg grating temperature sensor fabrication. IEEE Sensors Journal 2007; 7(4) 86-591.

[5] Zhao, Y., Zhao, H. W., Zhang, X. Y., Meng, Q. Y., and Yuan, B. A Novel double-arched-beam-based fiber Bragg grating sensor for displacement measurement. IEEE Photonics Technology Letters 2008; 20(15) 1296-1298.

[6] Jin, L., Zhang, W., Zhang, H., Liu, B., Zhao, J., Tu, Q., Kai, G., and Dong, X. An embedded FBG sensor for simultaneous measurement of stress and temperature. IEEE Photonics Technology Letters 2006; 18(1) 154-156.

[7] Yeh, C. H., Lin, M. C., Lee, C. C., and Chi, S. Fiber Bragg grating-based multiplexed sensing system employing fiber laser scheme with semiconductor optical amplifier. Japanese Journal of Applied Physics 2005; 44(9) 6590-6592.

[8] Chung, W. H., Tam, H. Y., Wai, P. K. A., and Khandelwal, A. Time- and wavelength-division multiplexing of FBG sensors using a semiconductor optical amplifier in ring cavity configuration. IEEE Photonics Technology Letters 2005; 17(12) 2709-2711.

[9] Yeh, C. H., and Chi, S. Fiber-fault monitoring technique for passive optical networks based on fiber Bragg gratings and semiconductor optical amplifier. Optics Communications 2006; 257(2) 306-310.

[10] Peng, P. C., Lin, W. P., and Chi, S. A self-healing architecture for fiber Bragg sensor network. Proceeding of Sensors 2004; 60-63.

[11] Wu, C. Y., Feng, K. M., Peng, P. C., and Lin, C. Y. Three-dimensional mesh-based multipoint sensing system with self-healing functionality. IEEE Photonics Technology Letters 2010; 22(8) 565-567.

[12] ITU-T, Recommendation G. 984.1 (2003): Gigabit-capable passive optical network (GPON): General Characteristics.

[13] Zhang, L., Liu, Y., Wiliams, J. A. R., and Bennion, I. Enhanced FBG strain sensing multiplexing capacity using combination of intensity and wavelength dual-coding technique. IEEE Photonics Technology Letters 1999; 11(12) 1638-1641.

IntechOpen